RSC Advances

PAPER

View Article Online
View Journal | View Issue

Cite this: *RSC Adv.*, 2017, **7**, 18132

Pyridinium 5-aminothiazoles: specific photophysical properties and vapochromism in halogenated solvents†

Kirara Yamaguchi, [a] Toshiaki Murai, *[a] Yuki Tsuchiya, [a] Yohei Miwa, [a] Shoichi Kutsumizu, [a] Takahiro Sasamori [b] and Norihiro Tokitoh [b]

Received 15th February 2017
Accepted 14th March 2017

DOI: 10.1039/c7ra01896g

rsc.li/rsc-advances

Treatment of pyridyl-5-aminothiazoles (**1–4**) with alkyl triflates or benzyl iodide afforded the corresponding pyridinium 5-aminothiazoles (**5–10**), which exhibited bathochromically shifted absorption and fluorescence spectra relative to those of **1–4**. Moreover, the vapochromic properties of **5** specific to halogenated solvents were examined by powder X-ray diffraction analysis. *Pmma* films containing **5** can thus be used to detect halogenated solvents, especially CH_2Cl_2.

Molecular scaffolds consisting of a combination of electron-donating (D) and -accepting (A) moieties *via* azole rings are of great interest. In particular, the introduction of electron-donating substituents at the 5-position of the 2-pyridinium azole provides conformationally flexible D–A systems[1] that find applications in organic electronics,[2] chemosensors,[3] biosensors,[4] and as potential drug candidates.[5] We have recently reported the first thiazoles that contain a strongly electron-donating diarylamino group at the 5-position, and pyridyl groups at the 2-position.[6] A further alkylation of the pyridine moiety was expected to enhance the acceptor character to provide molecules showing bathochromically shifted absorption and emission spectra. Herein, we report the synthesis and photophysical properties of pyridinium 5-aminothiazoles. Moreover, their vapochromic properties[7,8] specific to halogenated solvents, were examined by powder X-ray diffraction studies.

We initially treated 5-aminothiazoles **1–4** with either methyl or butyl triflate, or benzyl iodide to afford the desired pyridinium salts (**5–10**) in moderate to high yields (Fig. 1). The alkylation and benzylation occurred selectively at the nitrogen atom of the pyridine ring, even though **1–4** contain three nitrogen atoms. Pyridinium thiazole **8** was also obtained by this method, despite the steric hindrance of the nitrogen atom of the pyridine moiety.

Single crystals of **5** were obtained from a CH_2Cl_2 solution of **5** upon adding hexane. The molecular structure of **5** was determined by a single-crystal X-ray diffraction analysis (Fig. 2 and Table S1†), which revealed a significantly twisted 5-diphenylamino group similarly to that in **1**. The methylation of thiazole **1** induced a decrease of the dihedral angles at the 2- and 4-positions, under a concomitant slight planarization of the thiazole core and the substituents at these positions. Single crystals of **5** were also obtained from a THF solution of **5** upon adding hexane, and the structure obtained from these crystals is

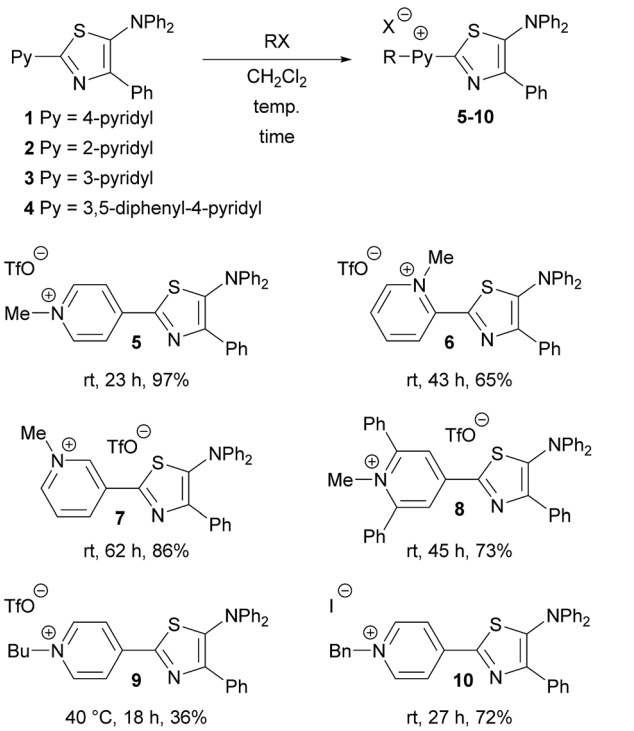

Fig. 1 Synthesis of pyridinium 5-aminothiazoles **5–10**.

[a]*Department of Chemistry and Biomolecular Science, Faculty of Engineering, Gifu University, Yanagido, Gifu 501-1193, Japan. E-mail: mtoshi@gifu-u.ac.jp; Fax: +81-58-293-2614; Tel: +81-58-293-2614*

[b]*Institute for Chemical Research, Kyoto University, Gokasho, Uji, Kyoto 611-0011, Japan*

† Electronic supplementary information (ESI) available: Experimental procedures, ^{1}H- and ^{13}C-NMR spectra, elemental analysis data, X-ray crystallographic data of reaction products. CCDC 1530518 and 1530519. For ESI and crystallographic data in CIF or other electronic format see DOI: 10.1039/c7ra01896g

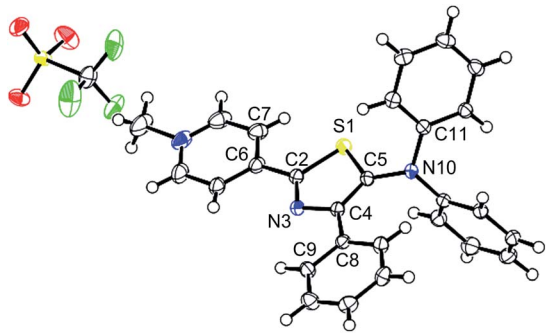

Fig. 2 The molecular structure for **5** (thermal displacement parameters set at 50% probability): selected dihedral angles (°) and bond lengths (Å): S1–C2–C6–C7 4.6(3), N3–C4–C8–C9 2.3(2), S1–C5–N10–C11 53.6(2), C2–C6 1.469(2), C4–C8 1.477(2), C5–N10 1.408(2), N10–C11 1.428(2).

virtually identical to that extracted from the crystals from CH_2Cl_2 (Fig. S1 and Table S2†).

The photophysical properties of **1–10** were measured in solution ($CHCl_3$ and THF) and in the solid state (Fig. 3 and S2, Table S3†). The absorption and fluorescence maxima of **1–4** shifted bathochromically upon conversion into the pyridinium salts (**5–10**). For example, the absorption maximum of **5** (λ_{abs} = 510 nm) in $CHCl_3$ was bathochromically shifted ($\Delta\lambda_{5/1}$ = 116 nm) relative to that of **1** (λ_{abs} = 394 nm) (Fig. 3a). The absorption wavelengths of **6** ($\Delta\lambda_{6/2}$ = 96 nm), **7** ($\Delta\lambda_{7/3}$ = 72 nm), and **8** ($\Delta\lambda_{8/4}$ = 113 nm) in $CHCl_3$ were also bathochromically shifted relative to the neutral starting materials. Thus, among the three regioisomers, *i.e.*, the isomers that contain 2-, 3-, or 4-pyridyl substituents at the 2-positions of the thiazoles, the alkylation of the 4-pyridyl group had the most profound impact on the photophysical properties. The pyridinium thiazoles with a butyl group (**9**; λ_{abs} = 510 nm) or a benzyl group (**10**; λ_{abs} = 517 nm) on the pyridyl nitrogen atoms showed similar absorption spectra in $CHCl_3$ to that of **5** with a methyl group. This result indicates that the nature of the substituents on the nitrogen atoms of the pyridinium thiazoles have little impact on the photophysical properties. Additionally, **5**, **9**, and **10** showed virtually identical fluorescence emissions (λ_{abs} = 650 nm) in $CHCl_3$ (Fig. 3b). All alkylated thiazoles (**5–10**) showed longer-wavelength emissions than those of the corresponding thiazoles (**1–4**). Although their fluorescence quantum yields (Φ_F) were very low in solution, **5–8** showed higher Φ_F values in the solid state than in solution (Fig. S3 and Table S3†).

The absorption spectra of **5–10** were also examined in various other solvents, which revealed characteristic differences between halogen-free (acetone, acetonitrile, and methanol) and halogenated solvents [tetrachloromethane, bromoform, pentafluorobutane (PFB), dichloromethane, dichloroethane (DCE), and tetrachloroethane (TCE)] (Table 1).[9] The maximum absorption wavelength of **5** in halogen-free solvents (λ_{abs} = ~480 nm) was bathochromically shifted in fluorinated, brominated, and chlorinated solvents.[10] In halogen-free solvents, a 1×10^{-5} M solution of **5** is pale yellow (Fig. 4), while it is orange, pink, and purple in fluorinated, brominated, and chlorinated solvents, respectively. These results indicate that the solvent polarity is not the major factor influencing the spectra. For example, the longest absorption maxima of **5** were observed at 510 nm ($CHCl_3$), 526 nm (CH_2Cl_2), and 547 nm (TCE), although the polarity parameter $E_T(30)$[11] of these solvents increases in the order $CHCl_3$ (39.1) < TCE (39.4) < CH_2Cl_2 (40.7) (Fig. 5). However, the magnitude of the bathochromic shift appeared to

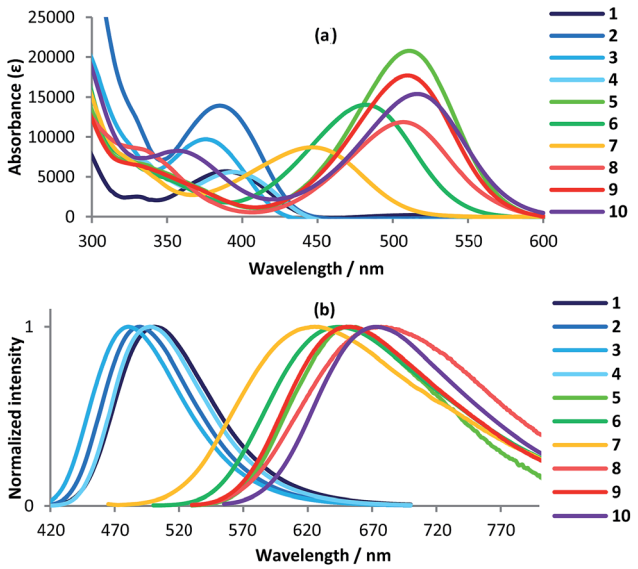

Fig. 3 (a) UV-vis absorption spectra of **1–10**; (b) emission spectra of **1–10**; [**1–10**] = 1×10^{-5} M in $CHCl_3$.

Table 1 Photophysical properties of **5** in various solvents; PFB: 1,1,1,3,3-pentafluorobutane, DCE: 1,2-dichloroethane, TCE: 1,1,2,2-tetrachloroethane; [**5**] = 1×10^{-5} M

		UV-vis		Fluorescence		
Solvent	$E_T(30)$	λ_{abs}/nm	log ε	λ_{em}[a]/nm	Φ_F[b]	Stokes shift/cm^{-1}
Acetone	42.2	476	4.01	—	—	—
CH_3CN	45.6	476	4.00	—	—	—
MeOH	55.4	482	3.93	—	—	—
CCl_4	32.4	484	3.39	596	0.07	3713 [108 nm]
$CHBr_3$	37.7	501	3.90	649	0.07	4552 [148 nm]
PFB	—	510	3.94	—	—	—
CH_2Cl_2	40.7	526	4.02	711	0.02	4947 [185 nm]
DCE	41.3	524	4.07	723	0.02	5253 [199 nm]
TCE	39.4	547	4.25	712	0.03	4237 [165 nm]

[a] Excited at the excitation wavelengths. [b] Absolute fluorescence quantum yield.

Fig. 4 Photographs of solutions of **5** in various solvents; [**5**] = 1×10^{-5} M.

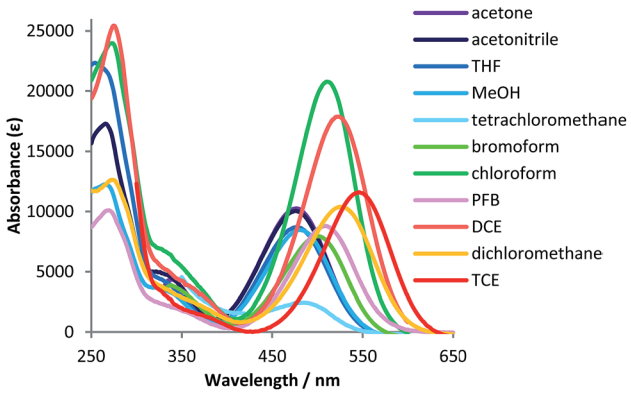

Fig. 5 UV-vis absorption spectra of **5** in various solvents; [**5**] = 1×10^{-5} M.

be governed by the number of halogen atoms per solvent molecule, *e.g.*, solvents with two halogen atoms shifted the absorption maximum of **5** to longer wavelengths than solvents with one halogen atom. Depending on the solvent, the fluorescence spectra of **5** in halogenated solvents exhibited emissions at λ_{em} = 596–723 nm (Fig. S4†). The Stokes shifts of **5** in halogenated solvents were also affected by the number of halogen atoms per solvent carbon atom, *i.e.*, the fluorescence emissions of **5** in CH_2Cl_2, DCE, and TCE occurred at longer wavelengths than those in CCl_4 and $CHBr_3$.

Interestingly, solid **5** exhibited reversible vapochromism toward halogenated solvents (Fig. 6 and Tables S5 and S6†).[11] When yellow solid **5** was exposed to CH_2Cl_2 vapor in a sealed glass case, its color quickly (2 min) changed to red. Opening the glass case and releasing the solvent vapor induced a rapid (~5 s) retroconversion to the yellow solid. When this red solid was exposed to CH_2Cl_2 vapor overnight, it changed to a red solution, which suggests that the solvent molecules may be intercalated into **5**, and that electrostatic interactions between the positively charged pyridinium moieties and halogen atoms may be present. This phenomenon was also observed for PMMA films prepared from **5** and PMMA pellets (Fig. S6†). After short (2 min) exposure to CH_2Cl_2 vapor, PMMA films containing **5** clearly turned red, and rapidly retroconverted to yellow upon opening the glass case. Exposure of **5** to TCE vapor also induced a similar color change from a yellow solid to a red solid (2 min), or to a red solution (overnight). However, in contrast to CH_2Cl_2 after opening the glass case and releasing the TCE vapor, the red solution converted only slowly (>2 min) back to the original yellow solid, while the color change is clearly visible with CH_2Cl_2. The discrepancy with respect to the rate of retroconversion should most likely be attributed to the difference in boiling point of the solvents. Nevertheless, dropping a CH_2Cl_2-:H_2O solution (1 : 1, v/v) on to a PMMA film containing **5** led to a swift color change, *i.e.*, such films can easily detect these solvents. In contrast, **5** did not show vapochromism in the presence of CCl_4 and PFB under similar conditions (Table S5†). When THF, MeOH, or DCE were used, the yellow solid of **5** turned to an orange solid overnight. Vapors of $CHCl_3$ and $CHBr_3$ changed the yellow solid of **5** into a red solid.

To compare the effects of halogenated and halogen-free solvents, the absorption spectra of solutions of **5** were measured. When 0.1–1.5 mL of $CHCl_3$ were added to a THF solution of **5** ([**5**] = 1×10^{-5} M, 2.5 mL), the longest absorption maximum shifted to a longer wavelength ($\Delta\lambda_{abs}$ = 18 nm) (Fig. S7†), while the addition of 0.1–1.5 mL of THF to a solution of **5** in $CHCl_3$ (2.5 mL) shifted the longest absorption maximum to shorter wavelengths ($\Delta\lambda_{abs}$ = 11 nm) (Fig. S8†). As the quantities of $CHCl_3$ and THF added are almost equivalent, $CHCl_3$ seems to change the photophysical properties more efficiently compared to THF.

Subsequently, we measured powder X-ray diffraction patterns of **5** in order to determine solvent-specific packing structures (Fig. 7, S9, and S10; Tables S7 and S8†). Column chromatography furnished **5** as a yellow solid, which was used after drying under reduced pressure. Samples containing THF and CH_2Cl_2 were generated by a solution-cast method followed by drying under atmospheric conditions. The thus obtained solid samples showed different patterns in the low-angle region. These results suggest that their packing structures are very different from each other. Therefore, packing structures of solid **5** should vary with the absorbed solvent. Based on the powder X-ray diffraction analysis, **5** crystallizes in the absence of any solvents in the relatively simple $P\bar{1}$ space group (Fig. S11†), whereas in the presence of THF, **5** includes THF molecules and crystallizes in the $C2/c$ (#15) space group (Fig. S12†). Moreover, the distance between the thiazole molecules shortened in the presence of THF.

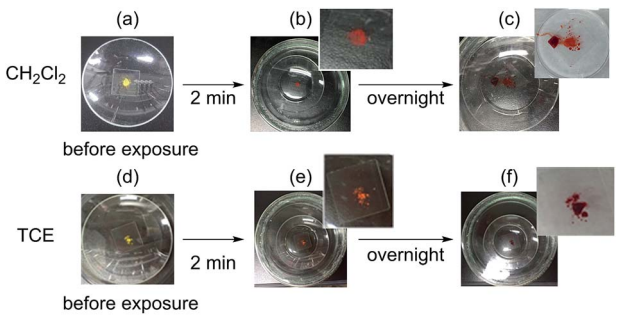

Fig. 6 Photographs of solid **5** sealed glass cases in the presence of CH_2Cl_2 (a–c) or TCE (d–f) vapor; diagonally offset inset photographs represent magnifications; (a and d) prior to exposure of **5** to solvent vapors; (b and e) after exposing **5** for two minutes to solvent vapor; (c and f) after exposing **5** to solvent vapor overnight.

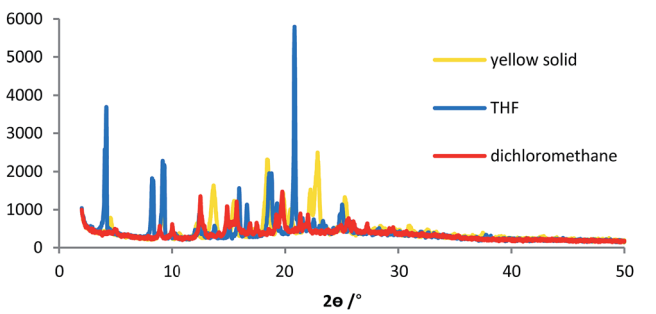

Fig. 7 Powder X-ray diffraction patterns of **5**; yellow solid **5** in the absence of solvents (yellow); solid **5** obtained from THF solution casting (blue), and solid **5** obtained from CH_2Cl_2 solution casting (red).

In conclusion, pyridinium 5-aminothiazoles bearing methyl, butyl, or benzyl groups on the pyridyl nitrogen atoms (**5–10**) were synthesized for the first time. These pyridinium thiazoles showed absorption in the visible region and red fluorescence in solution and in the solid state. In particular, the longest-wavelength absorption maximum of **5–10** exhibited specific bathochromic shifts in halogenated solvents. Moreover, **5** showed a reversible vapochromism upon exposure to vapors of CH_2Cl_2 and TCE. Powder X-ray diffraction patterns revealed that the packing structures of **5** change depending on the nature of the solvent molecules incorporated into the crystals. Furthermore, the addition of $CHCl_3$ to a THF solution of **5** caused a stronger shift of its absorption maximum than the addition of THF to a $CHCl_3$ solution of **5** under otherwise similar conditions. This phenomenon and the reversible vapochromism observed in PMMA films containing **5** should find applications in the detection of halogenated solvents, especially CH_2Cl_2.[12] Further studies on the applications of pyridinium 5-*N*-arylaminothiazoles that are responsive towards metals and solvents are currently in progress in our laboratory.

Notes and references

1 (*a*) V. V. Volchkov, G. H. B. Hoa, J. A. Kossanyi, S. P. Gromov, M. V. Alfimov and B. M. Uzhinov, *J. Phys. Org. Chem.*, 2005, **18**, 21–25; (*b*) A. V. V. Volchkov, G. V. Dem'yanov, M. V. Rusalov and T. I. Syreishchikova, *Russ. J. Gen. Chem.*, 2005, **75**, 790–794.

2 D. Svechkarev, D. Kolodezny, S. Mosquera-Vázquez and E. Vauthey, *Langmuir*, 2014, **30**, 13869–13876.

3 (*a*) M.-H. Zheng, J.-Y. Jin, W. Suna and C.-H. Yan, *New J. Chem.*, 2006, **30**, 1192–1196; (*b*) L.-L. Li, H. Sun, C.-J. Fang, J. N. Xu, J.-Y. Jin and C.-H. Yan, *J. Mater. Chem.*, 2007, **17**, 4492–4498; (*c*) Z.-X. Li, W. Sun, Y.-F. Yue, M.-H. Zheng, C.-H. Xu, J.-Y. Jin, C.-J. Fang and C.-H. Yan, *Tetrahedron Lett.*, 2007, **48**, 7675–7679; (*d*) Z.-X. Li, C.-H. Xu, W. Sun, Y.-C. Bai, C. Zhang, C.-J. Fanga and C.-H. Yan, *New J. Chem.*, 2009, **33**, 853–859; (*e*) S. Yamaguchi, H. Hosoi, M. Yamashita, P. Sen and T. Tahara, *J. Phys. Chem. Lett.*, 2010, **1**, 2662–2665; (*f*) S. Pajk, *Tetrahedron Lett.*, 2014, **55**, 6044–6047; (*g*) X. Ma, Y. Wang, T. Zhao, Y. Li, L.-C. Su, Z. Wang, G. Huang, B. D. Sumer and J. Gao, *J. Am. Chem. Soc.*, 2014, **136**, 11085–11092.

4 (*a*) Q. Wang, E. I. Zimmerman, A. Toutchkine, T. D. Martin, L. M. Graves and D. S. Lawrence, *ACS Chem. Biol.*, 2010, **5**, 887–895; (*b*) C. W. Cunningham, A. Mukhopadhyay, G. H. Lushington, B. S. J. Blagg, T. E. Prisinzano and J. P. Krise, *Mol. Pharm.*, 2010, **7**, 1301–1310; (*c*) B. Dumat, G. Bordeau, E. Faurel-Paul, F. Mahuteau-Betzer, N. Saettel, M. Bombled, G. Metgé, F. Charra, C. Fiorini-Debuisschert and M.-P. Teulade-Fichou, *Biochimie*, 2011, **93**, 1209–1218; (*d*) K. Zhou, H. Liu, S. Zhang, X. Huang, Y. Wang, G. Huang, B. D. Sumer and J. Gao, *J. Am. Chem. Soc.*, 2012, **134**, 7803–7811; (*e*) Q. Wang, M. A. Priestman and D. S. Lawrence, *Angew. Chem., Int. Ed.*, 2013, **52**, 2323–2325; (*f*) R. Schneider, A. Gohla, J. R. Simard, D. B. Yadav, Z. Fang, W. A. L. van Otterlo and D. Rauh, *J. Am. Chem. Soc.*, 2013, **135**, 8400–8408; (*g*) B. Dumat, E. Faurel-Paul, P. Fornarelli, N. Saettel, G. Metgé, C. Fiorini-Debuisschert, F. Charra, F. Mahuteau-Betzer and M.-P. Teulade-Fichou, *Org. Biomol. Chem.*, 2016, **14**, 358–370; (*h*) O. Brun, J. Agramunt, L. Raich, C. Rovira, E. Pedroso and A. Grandas, *Org. Lett.*, 2016, **18**, 4836–4839.

5 (*a*) M. Kitamatsu, T. Yamamoto, M. Futami and M. Sisido, *Bioorg. Med. Chem. Lett.*, 2010, **20**, 5976–5978; (*b*) Y. Martín-Cantalejo, B. Sáez, M. I. Monterde, M. T. Murillo and M. F. Braña, *Eur. J. Med. Chem.*, 2011, **46**, 5662–5667; (*c*) M. Manal, K. Arul, A. K. Anjana and K. Remya, *Int. J. Curr. Pharm. Res.*, 2014, **6**, 22–26; (*d*) K. Yokoo, K. Yamawaki, Y. Yoshida, S. Yonezawa, Y. Yamano, M. Tsuji, T. Hori, R. Nakamura and K. Ishikura, *Eur. J. Med. Chem.*, 2016, **124**, 698–712.

6 (*a*) K. Yamaguchi, T. Murai, S. Hasegawa, Y. Miwa, S. Kutsumizu, T. Maruyama, T. Sasamori and N. Tokitoh, *J. Org. Chem.*, 2015, **80**, 10742–10756; (*b*) K. Yamaguchi, T. Murai, J.-D. Guo, T. Sasamori and N. Tokitoh, *ChemistryOpen*, 2016, **5**, 434–438.

7 (*a*) O. S. Wenger, *Chem. Rev.*, 2013, **113**, 3686–3733; (*b*) C. Reus and T. Baumgartner, *Dalton Trans.*, 2016, **45**, 1850–1855.

8 (*a*) R. Matsushima, N. Nishimura and Y. Kohno, *Chem. Lett.*, 2003, **32**, 260–261; (*b*) R. Matsushima, N. Nishimura, K. Goto and Y. Kohno, *Bull. Chem. Soc. Jpn.*, 2003, **76**, 1279–1283; (*c*) M. Taneda, H. Koyama and T. Kawato, *Chem. Lett.*, 2007, **36**, 354–355; (*d*) E. Takahashi, H. Takaya and T. Naota, *Chem.–Eur. J.*, 2010, **16**, 4793–4802; (*e*) S. Yamada, A. Katsuki, Y. Nojiri and Y. Tokugawa, *CrystEngComm*, 2015, **17**, 1416–1420; (*f*) H. Naito, Y. Morisaki and Y. Chujo, *Angew. Chem., Int. Ed.*, 2015, **54**, 5084–5087; (*g*) P. S. Hariharan, D. Moon and S. P. Anthony, *J. Mater. Chem. C*, 2015, **3**, 8381–8388; (*h*) C. Peebles, C. D. Wight and B. L. Iverson, *J. Mater. Chem. C*, 2015, **3**, 12156–12163; (*i*) A. Sakon, A. Sekine and H. Uekusa, *Cryst. Growth Des.*, 2016, **16**, 4635–4645.

9 (*a*) A. Laguna, T. Lasanta, J. M. López-de-Luzuriaga, M. Monge, P. Naumov and M. E. Olmos, *J. Am. Chem. Soc.*, 2010, **132**, 456–457; (*b*) G. Park, H. Yang, T. H. Kim and J. Kim, *Inorg. Chem.*, 2011, **50**, 961–968; (*c*) H. Imoto, S. Tanaka, T. Kato, T. Yumura, S. Watase, K. Matsukawa and K. Naka, *Organometallics*, 2016, **35**, 3647–3650.

10 (*a*) Y. Ooyama, K. Kushimoto, Y. Oda, D. Tokita, N. Yamaguchi, S. Inoue, T. Nagano, Y. Harima and J. Ohshita, *Tetrahedron*, 2012, **68**, 8577–8580; (*b*) Y. Ooyama, Y. Oda, T. Mizumo and J. Ohshita, *Tetrahedron*, 2013, **69**, 1755–1760.

11 C. Reichardt, *Solvents and Solvent Effects in Organic Chemistry*, Wiley-VCH, Weinheim, Germany, 1988.

12 The importance of the development of the chemosensors to detect halogenated solvents has been reported elsewhere. For examples, see: (*a*) A. M. Alhuthali and I.-M. Low, *Polym.-Plast. Technol. Eng.*, 2013, **52**, 921–930; (*b*) T. Permpool, A. Sirivat, D. Aussawasathien and L. Wannatong, *Mater. Res.*, 2013, **16**, 1020–1029; (*c*) L. Dai, D. Wu, Q. Qiao, W. Yin, J. Yin and Z. Xu, *Chem. Commun.*, 2016, **52**, 2095–2098.